scientific reports

Check for updates

OPEN

Study of payload calculation and motion prediction for unpowered diving and floating of deep-sea manned submersible

Zhonghui Hu[1,2,3]✉, Cong Ye[1,2,3], Shuai Liu[1,2,3] & Wenxin Qu[1,2,3]

The preferred method of diving and floating for deep-sea manned submersibles is unpowered. This method has the potential to significantly reduce the energy expenditure of the submersible, extend the operational time of the submersible underwater, and is a fundamental aspect of the submersible's overall underwater operational capability. Environmental parameters, including seawater density and pressure, as well as the displacement volume of the submersible, fluctuate with depth. This results in a discrepancy between the calculated weights of the submersible diving ballast and floating ballast and the actual requirements. The weight of the diving ballast and floating ballast has a certain effect on the speed of the manned submersible during the processes of diving and floating. Therefore, conducting research into the matching calculation and motion prediction methods for unpowered diving ballast and floating ballast is highly practical for engineering. This paper presents a mathematical model of unpowered diving and floating motion for a manned submersible. It analyzes the forces acting on the submersible and establishes a method for matching ballast and predicting motion during unpowered diving and floating motions in deep water. The feasibility and effectiveness of the method described in this paper are verified and its suitability for engineering applications is demonstrated by comparing and analyzing the sea trial data with those of the "Jiao Long" manned submersible and the "Shen Hai Yong Shi" manned submersible.

Keywords Deep-sea manned submersible, Unpowered, Diving, Floating, Ballast, Prediction

Manned submersibles permit professionals to engage in the field to leverage their subjectivity and creativity fully and are an indispensable component of the equipment utilized for deep-sea access, exploration, development, and protection[1]. As a result of scientific and technological progress, deep-sea manned submersibles have become a key frontier and a dominant area of marine development technology, driving significant advances in deep-sea exploration capabilities[2–11]. This has attracted considerable interest from countries around the globe. The development of manned submersibles and related technologies has a longer history. A variety of deep-sea manned submersibles have been developed and deployed, including the American "Alvin"[12], the Russian "MIR-1" and "MIR-2"[3,13], the Japanese "Shinkai 6500"[14], and the French "Nautile"[5]. Notably, the "Alvin" successfully participated in and completed a number of missions, including the search for crashed hydrogen bombs, the exploration of hydrothermal areas on the seabed, and the search for the wreckage of the Titanic. The "Shinkai 6500" has successfully completed tasks such as the investigation of oceanic slopes and large faults at water depths of 6500 m. The "MIR-1" and "MIR-2" have accomplished such tasks as nuclear radiation detection on a wrecked nuclear submarine and the "Arctic-2007" marine scientific expedition[15]. The advent of deep-sea manned submersibles, particularly those capable of operating at depths exceeding 11,000 m, has given rise to a new era of scientific and technological competition. In 2012, the "Deepsea Challenger" manned submersible, developed by the U.S. Cameron team, reached a depth of 10,898 m in the Marianas Trench, establishing a new record for the depth of a single person's dive[16]. On November 10, 2020, the China-developed "Fen Dou Zhe" full-depth manned submersible successfully completed a dive to a depth of 10,909 m in the Mariana Trench, establishing a new national record for manned deep diving[17].

The duration of underwater operations represents a crucial metric for assessing the operational capacity of deep-sea manned submersibles. The capacity for deep-sea manned submersibles to carry energy is constrained

[1]China Ship Scientific Research Center, Wuxi 214082, China. [2]State Key Laboratory of Deep-Sea Manned Vehicles, Wuxi 214082, China. [3]Taihu Laboratory of Deepsea Technological Science, Wuxi 214082, China. ✉email: hzh_702@163.com

by the combined weight and size of the vehicle. To ensure an adequate operational lifespan, deep-sea manned submersibles typically employ unpowered diving and floating techniques[18–20]. This type of diving and floating movement enables the manned submersible to complete diving and floating at the expected speed through diving ballast and floating ballast, which can significantly reduce the energy consumption of the manned submersible and increase the operating time of the manned submersible underwater. It is one of the fundamental bases for the underwater operation capability of deep-sea manned submersibles. However, environmental parameters, such as seawater density and pressure, change with depth. These factors have a nonnegligible effect on the force exerted on the deep-sea manned submersible, resulting in a mismatch between the weights of the diving ballast and floating ballast of deep-sea manned submersibles and the anticipated outcomes. This discrepancy affects the equilibrium of the deep-sea manned submersible underwater and the control of the speed of the downward and upward motions. Consequently, the analysis of load calculation and motion prediction for unpowered diving and floating of deep-sea manned submersibles is of significant importance.

This paper examines the impact of environmental parameters, including seawater pressure, temperature, salinity, and density, on the unpowered diving and floating motion of deep-sea manned submersibles. This paper introduces the concept of the volume compression rate and presents a methodology for predicting and matching ballast for unpowered diving and floating motion in deep-sea environments. The objective is to provide reliable technological means for the design of unpowered diving and floating motions in deep-sea manned submersibles. It has been demonstrated that the methodology can enhance the ability of the submersible to control the speed of unpowered diving and floating, ensure that the submersible has enough operating time underwater, and provide an important guarantee for the submersible's underwater operation.

Mathematical modeling of unpowered diving and floating motion

Hypothesis

The research work is carried out in the context of engineering applications. The hypothesis for simplified calculation is given in literature[21], as follows:

1. During the unpowered diving and floating motion of the submersible, only the variation of the velocity in the vertical direction is considered.
2. The unpowered diving and floating motion of a manned submersible is approximated as constant velocity motion, whereby the acceleration of the unpowered diving and floating motion is approximated to be zero.
3. In the calculation process, only the smooth dive phase and the smooth float phase of the manned submersible are considered.

Motion mathematical model

The forces acting on the manned submersible during unpowered diving and floating motions are illustrated in Fig. 1.

As illustrated in Fig. 1, the forces exerted on a manned submersible during its unpowered descent and ascent include gravity G (diving ballast and floating ballast not included, diving ballast and floating ballast considered additional forces), buoyancy B, hydrodynamic force F_d, and an additional force F_{ad}. the unpowered diving and floating motion of manned submersibles are in accordance with Newton's second law. Because the angular velocity of the manned submersible is zero during steady-state motion and other factors, the analysis considers only heave motion and assumes zero pitch and roll angles (theta = phi = 0). In addition any possible underwater current is ignored. The mathematical model of the unpowered diving and floating motion of the manned submersible is obtained as follows:

$$\vec{G} + \vec{B} + \vec{F}_d + \vec{F}_{ad} = M\vec{a} \tag{1}$$

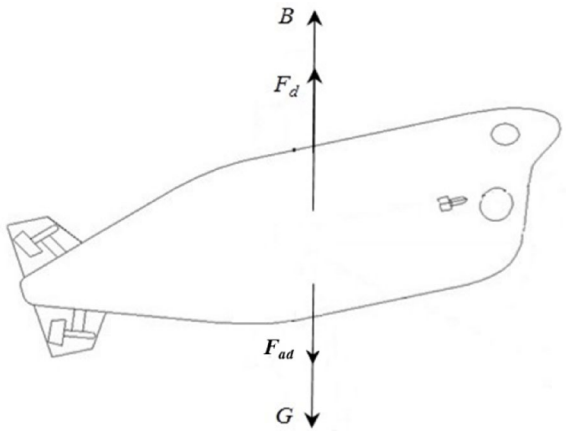

Fig. 1. Force analysis.

In this context, M represents the mass of the manned submersible, whereas a denotes the acceleration of the manned submersible during its diving and floating motions.

In conjunction with the assumptions outlined in Section "Hypothesis", Eq. (1) can be further simplified as follows:

$$\vec{G} + \vec{B} + \vec{F}_d + \vec{F}_{ad} = 0 \tag{2}$$

Gravity *G*

The weights of a manned submersible can be classified into two categories: fixed weights and variable weights. In this context, variable weights encompass the weights of personnel, cabin consumables, and other relevant items. The gravitational force G acting on a manned submersible can be expressed as:

$$G = (M_0 + M_c) \cdot g \tag{3}$$

In this context, M_0 represents the fixed weight of the submersible, whereas M_c denotes the variable weight of the submersible.

Given the temporal and spatial variability of the global distribution of the gravity field[22,23], gravity anomalies are expected to undergo changes during the diving and floating motions of deep-sea manned submersibles. The effect of gravity anomalies on the combined force of gravity and buoyancy in abyssal profiles has been analyzed in the literature[24]. The results of the analysis indicate that gravity anomalies generally do not exceed -1000 mGal and affect only the combined force of gravity and buoyancy, i.e., gravity anomalies bring about a change in the combined force of no more than 1 N. The net buoyancy of a submersible during dive and ascent is typically measured in thousands of Newtons, and changes in the gravitational acceleration g have a negligible effect on deep-sea manned submersibles during diving and floating. Accordingly, the acceleration of gravity g is taken as 9.80655 m/s^2 in the calculations.

Buoyancy *B*

The force of buoyancy experienced by a manned submersible while diving and floating can be described as follows:

$$\begin{cases} B = \rho(h)\, g\, (1 - k(h))\, V_0 \\ k(h) = k_1(h) + k_2(h) + k_3(h) \end{cases} \tag{4}$$

In this context, g represents the gravitational acceleration, V_0 denotes the displaced volume when the manned submersible is completely submerged at the start of the dive at the sea surface. k is the coefficient of displaced volume loss, k is the displacement volume loss coefficient, which is defined as the ratio of the displaced volume lost by the submersible to V_0. k_1 is used to denote the displaced volume loss coefficient of the pressure-resistant structure, which is defined as the ratio of the displaced volume lost by the pressure-resistant structure of submersible to V_0. k_2 is used to denote the displaced volume loss coefficient of the buoyant material, which is defined as the ratio of the displaced volume lost by the buoyant material of submersible to V_0. k_3 is used to denote the displaced volume loss coefficient of the displaced volume loss coefficient of the pressure-compensating component, which is defined as the ratio of the displaced volume lost by the pressure-compensating component of submersible to V_0. h represents the current depth of the submersible.

From the literature[21,25], it can be seen that when the submersible starts diving from the sea surface, the displacement volume lost by the submersible is zero, i.e. the initial value of k is zero. As the depth of dive increases, the displaced volume lost by the submersible varies essentially linearly with depth, i.e. k varies linearly with depth. Section "Calculation of the displaced volume loss coefficient" of this paper lists the detailed calculations for k.

The environmental parameters of the marine environment, including seawater density and pressure, are subject to variations with changes in ocean depth. On the one hand, alterations in the density of seawater result in corresponding changes in the buoyancy force experienced by the manned submersible. On the other hand, seawater pressure causes a change in the volume of water discharged from a manned submersible. Consequently, to accurately calculate the buoyancy force exerted on a manned submersible, it is essential to obtain precise data regarding the density of seawater and the volume of water discharged.

Calculation of seawater density

The density of seawater varies with depth. Figure 2 illustrates the variation in seawater density with depth, as measured during the D44 dive in the 5000-m sea trial of the "Jiao Long" manned submersible.

As illustrated in Fig. 2, the density of seawater increases with depth. The variation in seawater density is significant in the range of water depths from 0–400 m. As the depth of seawater exceeds 400 m, the gradient of change in seawater density decreases and becomes approximately linear with depth. The density of seawater at a depth of 5000 m was observed to have increased by 2.88% in comparison to the density of seawater at the surface. If the volume of a manned submersible remains unaltered, the buoyancy force on the manned submersible increases by 2.88%. Extrapolation indicates that at a water depth of 11,000 m, the buoyancy force on a deep-sea manned submersible will increase by approximately 5.68%. The alterations in the buoyancy force experienced by a manned submersible as a result of fluctuations in seawater density are not inconsequential and must be considered when predicting the unpowered diving and floating motion of a manned submersible and the required ballast weights.

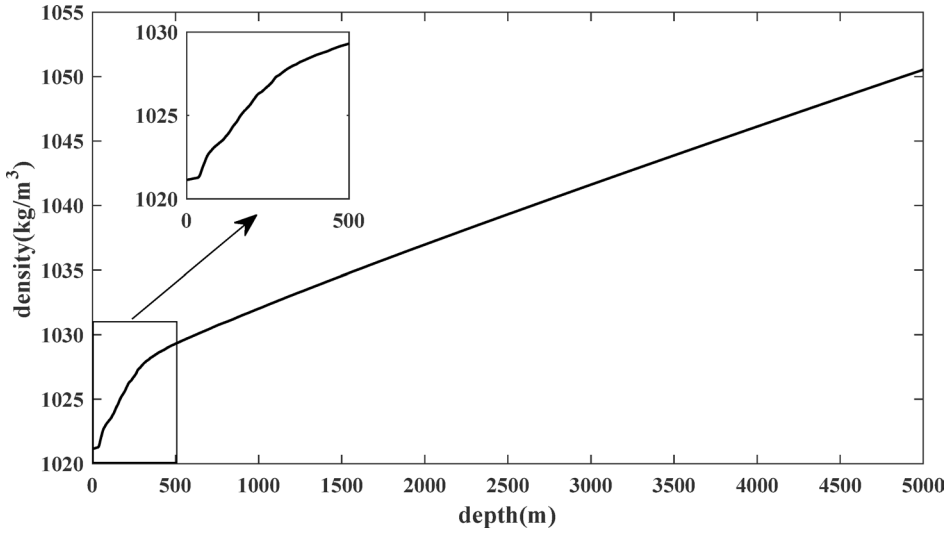

Fig. 2. Density curve of sea water with depth.

The density of seawater can be calculated indirectly by employing the equation of state of seawater[26,27]. This equation incorporates the influences of seawater temperature, salinity, and pressure on seawater density. The range of application of this equation is as follows: temperature, -2 to 40 °C; salinity, 0–42%; and seawater pressure, 0–100 MPa. The Mariana Trench represents the deepest point in the global ocean, with a depth exceeding 11,000 m and a seawater pressure in excess of 100 MPa. These conditions exceed the limits of applicability of the aforementioned equation.

A preliminary conclusion drawn from the literature[24] is that the equation has the potential to calculate the density of seawater for seawater pressures exceeding 100 MPa. This paper presents an analysis of the physical parameters of seawater in ocean profiles on the basis of empirical observations of the physical characteristics of seawater in the Mariana Trench. A methodology for calculating seawater temperature, salinity, and pressure is also proposed. On this basis, this paper determines the scope of application of the EOS80 seawater equation of state.

Pressure of seawater Considering the relationship between seawater pressure and depth, it can be posited that seawater pressure is a function of depth. In the analysis, seawater pressure is considered to be a polynomial function of depth. Based on the seawater pressure measurements taken in the vicinity of the Mariana Trench and the least squares method is used to identify the model parameters to obtain the equation for seawater pressure as follows:

$$P(h) = -1.2042 \times 10^{-11} h^3 + 2.4518 \times 10^{-6} h^2 + 1.0057h - 0.0041 \tag{5}$$

Equation 5 is identified from the real data of the Mariana Trench and is applicable to the position of the Mariana Trench. In the development of submersibles, in instances where the marine parameters of the operational sea area are unknown, this equation can be utilised to obtain the seawater pressure through approximate calculation. In the event that the marine parameters of the operational sea area are known, the seawater pressure can be obtained by calculating it based on the actual marine parameters.

Temperature of seawater Figure 3 shows the seawater temperature measurements taken in the vicinity of the Mariana Trench.

As shown in Fig. 3, there was a notable decline in the seawater temperature between depths of 0–600 m. At seawater depths between 600 and 3000 m, the rate of change in seawater temperature with depth decreases. At depths greater than 3000 m in the sea, the temperature of the seawater tends to increase gradually with depth. In the analysis, the seawater temperature is considered to be a polynomial function of depth. A segmented modeling approach is employed, whereby the model parameters are identified via the least squares method, which yields the following equation for the seawater temperature:

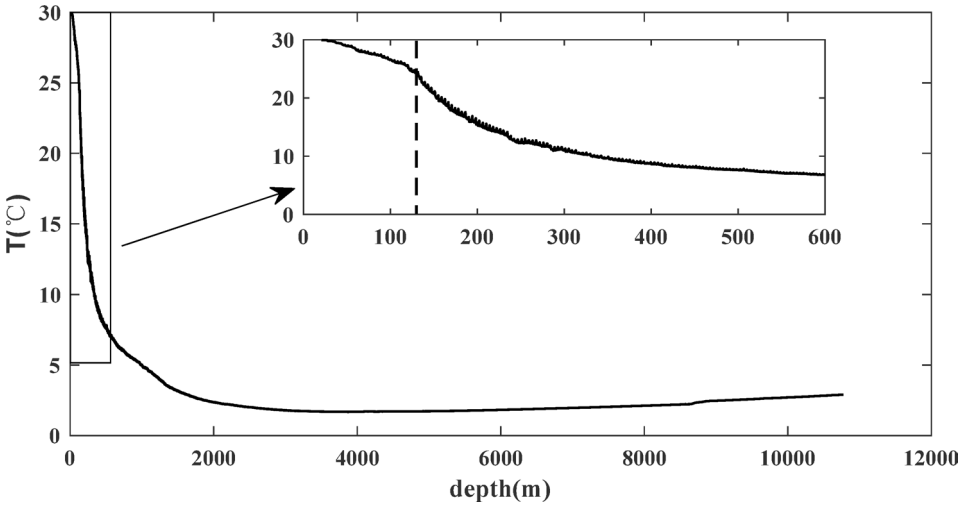

Fig. 3. Temperature curve of sea water with depth.

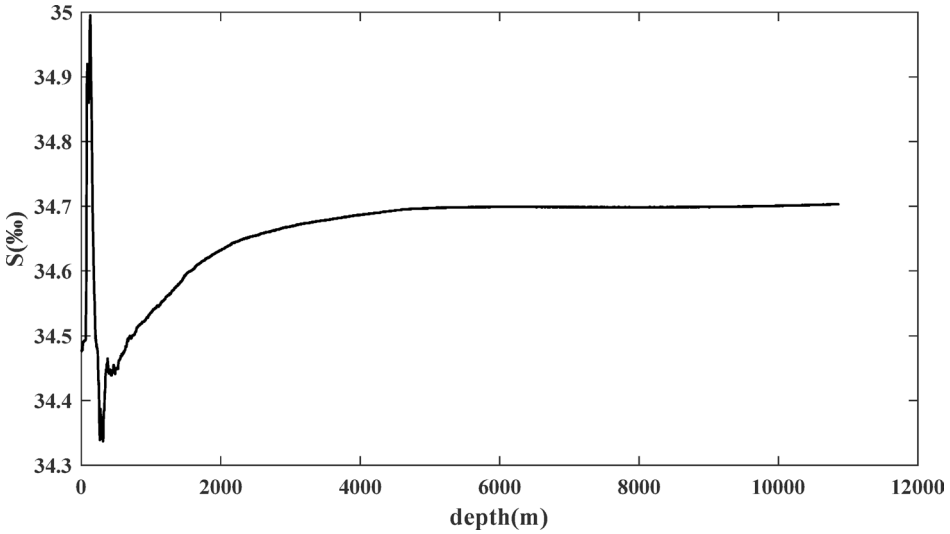

Fig. 4. Salinity curve of sea water with depth.

$$T(h) = \begin{cases} -1.0388 \times 10^{-7}h^4 + 3.0009 \times 10^{-5}h^3 - 3.0849 \times 10^{-3}h^2 \\ +8.5711 \times 10^{-2}h + 29.283 & 0 \le h \le 120m \\ -4.2072 \times 10^{-12}h^5 + 8.7097 \times 10^{-9}h^4 - 7.1766 \times 10^{-6}h^3 \\ +2.9913 \times 10^{-3}h^2 - 0.6563h + 72.066 & 120m < h \le 600m \\ 3.1102 \times 10^{-16}h^5 - 3.0766 \times 10^{-12}h^4 + 1.1245 \times 10^{-8}h^3 \\ -1.7531 \times 10^{-5}h^2 + 7.8089 \times 10^{-3}h + 6.1798 & 600m < h \le 3000m \\ -1.0405 \times 10^{-12}h^3 + 4.8673 \times 10^{-8}h^2 - 3.5345 \times 10^{-4}h \\ +2.4044 & 3000m < h \end{cases} \quad (6)$$

Salinity of seawater Figure 4 shows the seawater salinity measurements taken in the vicinity of the Mariana Trench.

As shown in Fig. 4, the salinity of the seawater surface is approximately 34.4‰. There is subsequently a marked decrease in the salinity of seawater with depth, reaching a minimum value at approximately 310 m, which is equivalent to 34.33‰. The salinity of seawater subsequently increases gradually with depth, reaching a relatively constant value of approximately 34.7‰ near 4700 m. In light of the findings of the aforementioned analysis, the following equation for calculating the salinity of seawater has been derived:

$$S(h) = \begin{cases} \left(4.538 \times 10^{-3}h + 34.4\right)‰ & 0 \le h \le 130m \\ \left(-3.667 \times 10^{-3}h + 35.467\right)‰ & 130m < h \le 310m \\ \left(\begin{array}{c} -4.5811 \times 10^{-16}h^4 + 1.0135 \times 10^{-11}h^3 - 7.7157 \times 10^{-8}h^2 \\ +2.6172 \times 10^{-4}h + 34.342 \end{array}\right)‰ & 310m < h \le 4700m \\ 34.7‰ & 4700m < h \end{cases} \tag{7}$$

Density of seawater In this work, the density of seawater at depths exceeding 10,000 m is calculated via the EOS80 seawater equation of state, which is based on the aforementioned calculation methods of seawater pressure, temperature and salinity. The results are presented in Fig. 5 and compared with the measured seawater density data.

As illustrated in Fig. 5, the density of seawater calculated by the EOS80 seawater equation of state is found to be in general agreement with the observed data. The root mean square error is 0.11 kg/m^3. In other words, the EOS80 seawater equation of state remains capable of accurately calculating seawater density when the seawater pressure exceeds 100 MPa. Accordingly, the EOS80 seawater equation of state is suitable for calculating seawater density at any depth in the ocean.

Calculation of the displaced volume loss coefficient

The "Alvin" manned submersible is used as an example to illustrate the location of typical components on a manned submersible, as shown in Fig. 6.

As shown in Fig. 6, a plethora of pressure-resistant structures, buoyancy materials and hydraulically compensated components are distributed on deep-sea manned submersibles. The displaced volume of these components of a deep-sea manned submersible is subject to variation in accordance with the prevailing seawater pressure.

As shown in Fig. 7, the pressure-resistant structures include spherical shell pressure-resistant structures and cylindrical shell pressure-resistant structures, which provide an atmospheric survival environment for personnel and equipment.

As shown in Fig. 8, buoyancy material is a kind of polymer-based solid material with low-density and high-strength. It provides buoyancy to the manned submersible.

As shown in Fig. 9, the pressure-compensating component is hydraulic pressure compensation devices for manned submersibles. Its main function is to ensure that the pressure of the hydraulic system on the manned submersible is greater than the external water pressure, ensuring the safety of the system. The pressure-compensating component has a built-in compression bladder, which ensures the reliability of the seal. And it provides a pre-pressure by means of a compression spring which enables the compensating pressure to be higher than the external water pressure, thus effectively preventing seawater backflow.

This paper introduces the concept of the displaced volume loss coefficient, denoted by k. In light of the compositional characteristics exhibited by components of deep-sea manned submersibles, the displaced volume loss coefficient k can be expressed as follows:

$$k = k_1 + k_2 + k_3 \tag{8}$$

In this context, symbols k_1, k_2, and k_3 are used to denote the displaced volume loss coefficient of the pressure-resistant structure, the displaced volume loss coefficient of the buoyant material, and the displaced volume loss coefficient of the pressure-compensating component, respectively.

The coefficient of displaced volume loss for pressure-resistant structures

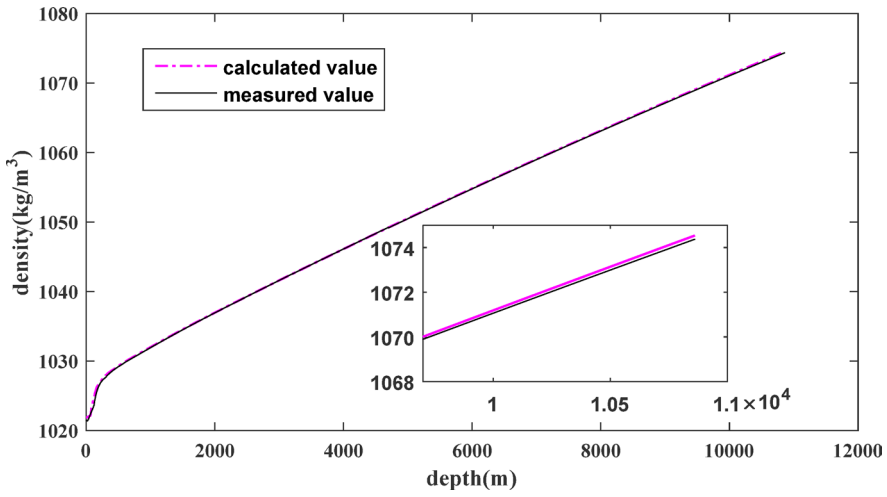

Fig. 5. Density curve of sea water with depth.

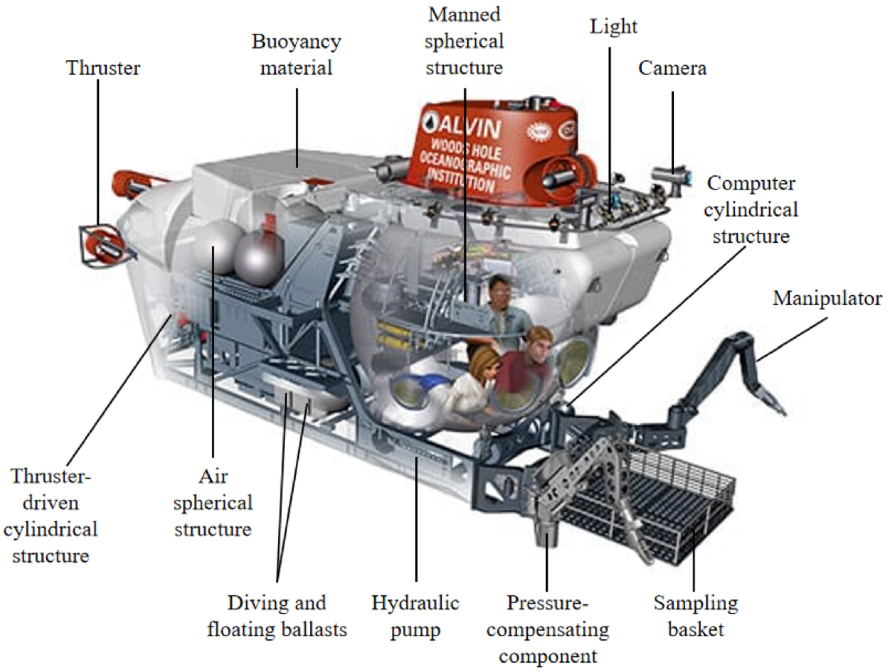

Fig. 6. Schematic diagram of typical component location[12].

Fig. 7. Schematic diagram of pressure-resistant structure[28].

The changes in displaced volume in pressure-resistant structures can be classified into two main categories: changes in the displaced volume of spherical shell pressure-resistant structures and changes in the displaced volume of cylindrical shell pressure-resistant structures. The primary pressure-resistant structures on manned submersibles can be classified into two categories according to their shape:

1. Spherical shells include manned tanks, adjustable ballast water tanks, high-pressure gas tanks, etc.
2. Cylindrical shells: power distribution tanks, computer tanks, hydroacoustic communication tanks, drive tanks, etc.

The displaced volume loss coefficient for pressure-resistant structures can be expressed as follows:

$$k_1 = k_{11} + k_{12} \tag{9}$$

In this context, k_{11} represents the displaced volume loss coefficient of the spherical shell pressure-resistant body, whereas k_{12} denotes the displaced volume loss coefficient of the cylindrical shell pressure-resistant body.

a. Displaced volume loss coefficient of the spherical shell pressure-resistant body

Fig. 8. Schematic diagram of buoyancy material[29].

Fig. 9. Schematic diagram of pressure-compensating component.

As documented in the literature[28], the ratio of mean radius to wall thickness of the spherical pressure-resistant structures of deep-sea manned submersibles is as follows: ratio of diameters ≥ 10. Accordingly, the spherical pressure-resistant structure can be approximated as a thin shell for the purpose of calculating deformation[30].

The internal pressure of the spherical shell is designated P_1.When a manned submersible dive commences, the displaced volume of the spherical shell can be expressed as follows:

$$V_{S0} = \frac{4\pi}{3}(R + t + \Delta r_{S0})^3 \tag{10}$$

In this context, R is the inner radius of the spherical shell, t is the thickness of the spherical shell, and Δr_{S0} is the radial deformation of the spherical shell, which can be expressed as follows:

$$\Delta r_{S0} = \frac{P_1(R + t/2)^2}{2Et}(1 - \mu) \tag{11}$$

In this context, P_1 is the internal pressure of the spherical shell, E is the Young's modulus of the material, and μ is the Poisson's ratio of the material.

When the manned submersible dives to a certain depth, the seawater pressure is P_2. At this point, each spherical shell of the manned submersible is subjected to both external pressure P_2 and internal pressure P_1. The displaced volume of the spherical shell can be expressed as follows:

$$V_{S1} = \frac{4\pi}{3}(R + t + \Delta r_{S1})^3 \tag{12}$$

In this context, Δr_{S1} represents the radial deformation of the spherical shell, which can be expressed as follows:

$$\Delta r_{S1} = \frac{(P_1 - P_2)R^2}{2Et}(1-\mu) \tag{13}$$

The reduction in the displaced volume of each spherical shell is as follows:

$$\Delta V_S = V_{S0} - V_{S1} \tag{14}$$

The displaced volume loss coefficient of the spherical shell pressure-resistant body is given by the following equation:

$$k_{11} = \frac{\sum \Delta V_{Si}}{V_0} \tag{15}$$

b. Displaced volume loss coefficient of the cylindrical shell pressure-resistant body

As documented in the literature[30], the ratio of mean radius to wall thickness of the cylindrical shell pressure-resistant structure of a deep-sea manned submersible is as follows: ratio of diameters < 10.Accordingly, the cylindrical shell pressure-resistant structure can be approximated as a thick-walled cylinder for the purpose of calculating deformation.

The internal pressure of the cylindrical shell is designated P_1.When a manned submersible dive commences, the displaced volume of the cylindrical shell can be expressed as follows:

$$V_{C0} = \pi(\mathrm{r}_1 + t + \Delta r_{C0})^2(l + \Delta l_{C0}) \tag{16}$$

In this context, r_1 signifies the inner radius of the cylindrical shell, Δr_{C0} signifies the radial deformation of the cylindrical shell, Δl_{C0} signifies the axial deformation of the cylindrical shell,l signifies the length of the cylindrical shell axis, and t signifies the thickness of the cylindrical shell.The quantity "Δr_{C0}" can be expressed as follows:

$$\Delta r_{C0} = \frac{2-\mu}{E} \times \frac{P_1 r_1^2 r_2}{r_2^2 - r_1^2} \tag{17}$$

The quantity "Δl_{C0}" can be expressed as follows:

$$\Delta l_{C0} = \frac{1-2\mu}{E} \times \frac{P_1 r_1^2 l}{r_2^2 - r_1^2} \tag{18}$$

In this context, r_2 represents the outer radius of the cylindrical shell, E is the Young's modulus of the material, and μ is the Poisson's ratio of the material.

When the submersible dives to a certain depth, the seawater pressure is P_2.At this point, each cylindrical shell of the manned submersible is subjected to both external pressure P_2 and internal pressure P_1. The displaced volume of the cylindrical shell can be expressed as follows:

$$V_{C1} = \pi(r_1 + t + \Delta r_{C1})^2(l + \Delta l_{C1}) \tag{19}$$

In this context, Δr_{C1} and Δl_{C1} represent the radial deformation and axial deformation of the cylindrical shell, respectively. The quantity "Δr_{C1}" can be expressed as follows:

$$\Delta r_{C1} = \frac{1-2\mu}{E} \times \frac{P_1 r_1^2 - P_2 r_2^2}{r_2^2 - r_1^2} r_2 + \frac{1+\mu}{E} \times \frac{P_1 - P_2}{r_2^2 - r_1^2} r_1^2 r_2 \tag{20}$$

The quantity "Δl_{C1}" can be expressed as follows:

$$\Delta l_{C1} = \frac{1-2\mu}{E} \times \frac{P_1 r_1^2 - P_2 r_2^2}{r_2^2 - r_1^2} l \tag{21}$$

The reduction in the displaced volume of each cylindrical shell is as follows:

$$\Delta V_C = V_{C0} - V_{C1} \tag{22}$$

The displaced volume loss coefficient of the cylindrical shell pressure-resistant body is given by the following equation:

$$k_{21} = \frac{\sum \Delta V_{Ci}}{V_0} \tag{23}$$

The coefficient of displaced volume loss for buoyant materials The buoyancy loss experienced by the buoyant material of a manned submersible is attributable primarily to two underlying factors: water absorption (equivalent conversion) and volume contraction of the buoyant material. The displaced volume loss coefficient for buoyant materials can be expressed as follows:

$$k_2 = k_{21} + k_{22} \tag{24}$$

In this context, k_{21} represents the displaced volume loss coefficient caused by the absorption of water of the buoyant material, whereas k_{22} represents the displaced volume loss coefficient caused by the volume contraction of the buoyant material.

a. Displaced volume loss caused by the absorption of water by buoyant materials

The water absorption fraction η of the buoyant material can be expressed as follows:

$$\eta = \frac{\Delta M_{bm}}{M_{bm}} = \frac{M_{bm1} - M_{bm0}}{M_{bm0}} = \frac{\rho \cdot \Delta V_{bm}}{\rho_{bm} \cdot V_{bm0}} \tag{25}$$

In this context, ΔM_{bm} denotes the change in mass of the buoyant material after water absorption, M_{bm0} denotes the mass of the buoyant material before water absorption, M_{bm1} denotes the mass of the buoyant material after water absorption, ρ_{bm} denotes the density of the buoyant material, ΔV_{bm} denotes the equivalent lost displaced volume of the buoyant material, and V_{bm0} denotes the initial displaced volume of the buoyant material.

The volume loss of buoyant material due to water absorption can be expressed as the coefficient of buoyancy loss, designated $k21$, which can be expressed as follows:

$$k_{21} = \Delta V_{bm} / V_0 = \left(\rho_{bm} \cdot V_{bm0} \cdot \eta\right) / \left(\rho \cdot V_0\right) \tag{26}$$

b. Displaced volume loss caused by volume contraction of the buoyant material

The volumetric shrinkage of a buoyant material subjected to high hydrostatic pressure is independent of the shape and volume of the material. It is related to the homogeneous hydrostatic pressure p and the volumetric elastic modulus K. The volume loss of buoyant material due to volume shrinkage can be expressed as the buoyancy loss coefficient, designated k_{22}, which can be expressed as follows:

$$k_{22} = -\frac{p}{K} \cdot \frac{V_{bm0}}{V_0} \tag{27}$$

The volumetric elastic modulus K can be expressed as follows:

$$K = \frac{E}{3\left(1 - 2\mu\right)} \tag{28}$$

In this context, E represents the Young's modulus of the buoyant material, whereas μ denotes the Poisson's ratio of the buoyant material.

The coefficient of displaced volume loss for the pressure-compensating component A significant number of pressure compensation components are utilized in the construction of deep-sea manned submersibles. The hydraulic fluid will undergo compression as a result of the action of seawater pressure. Concurrently, compensating components that utilize hydraulic fluids generate identical compression. This results in a reduction in the displacement volume of the manned submersible. The compression fraction of a hydraulic fluid is a function of seawater pressure and can be expressed as follows:

$$\eta_{hf} = \eta_{hf}\left(P\right) \tag{29}$$

The displaced volume loss coefficient of the pressure-compensating component can be expressed as follows:

$$k_3 = \eta_{hf} \cdot \frac{V_{hf0}}{V_0} \tag{30}$$

In this context, V_{hf0} represents the volume of hydraulic fluid at atmospheric pressure.

Hydrodynamic force F_d

The hydrodynamic forces acting on a deep-sea manned submersible can be expressed as follows:

$$F_d = \frac{1}{2}\rho L^2 U^2 \cdot C_Z \tag{31}$$

In this context, ρ represents the density of seawater, L denotes the characteristic length of the deep-sea manned submersible, U denotes the velocity in the dive and float directions, and C_z denotes the drag coefficients in the diving and floating directions. The drag coefficient, denoted by C_z, can be estimated in several ways. These include the use of empirical formulas, the application of numerical simulation, and the undertaking of modeling tests[31].

Additional force F_{ad}

In this work, the weights of the diving ballast and floating ballast are considered additional forces that act on deep-sea manned submersibles. The additional force can be expressed as follows:

$$F_{ad} = (M_1 g - \rho g V_1) + (M_2 g - \rho g V_2) \tag{32}$$

In this context, M_1 represents the weight of the floating ballast in air, M_2 denotes the weight of the diving ballast in air, V_1 signifies the displaced volume of the floating ballast, and V_2 indicates the displaced volume of the diving ballast.

Calculation procedure

The operation of diving and floating ballast is as follows.

Prior to dive, install the diving ballast and floating ballast on the deck of the mother ship to the mounting interface of the ballast release device. Deploy the submersible into the water. The submersible dives, and when it is about to reach the operation depth, the pilot releases the diving ballast through the ballast release device controlled by the control system in the manned tank. When completing the operation and need to float, the pilot in the manned tank through the control system to control the ballast release device to release the floating ballast.

Diving and floating ballast is a load weight block arranged underneath the side of the submersible. The diving ballast is used to achieve unpowered diving motion for deep-sea manned submersibles. The floating ballast is used to realize the unpowered floating motion of the deep-sea manned submersible. The computational solution flow for diving and floating motions with ballast matching is illustrated in Fig. 10. The calculations include the diving phase calculations and the floating phase calculations. The calculations are the same for both phases. The subsequent diving phase calculation is an exemplar of the calculation process. The calculation process is cyclical, with diving and floating ballast functioning as the cyclic variable. In the course of the calculations, the initial value of the weights of the diving ballast and floating ballast is set at zero. The setting is performed by the additional force step-up module. On the basis of the desired d depth, diving time and floating time, we forecast the diving and floating speed of the manned submersible in its current state. If the predicted speed meets the desired requirements, the calculation stops, and the weights of the current diving ballast and floating ballast become the weights of the diving ballast and floating ballast to be matched. If the predicted speed does not meet the desired requirements, the weights of the diving ballast and floating ballast must be increased further. Diving and floating ballast weights are increased in set increments by means of additional force step-up modules. The above calculation process is repeated until the diving and floating speeds meet the desired requirements, the calculation stops, and the current diving ballast and floating ballast weights become the diving ballast and floating ballast weights to be matched. The recurrence of calculations with depth as a variable is embedded within a singular calculation loop. The initial value of the depth is set to zero. Based on the parameters and depth values of the submersible, calculate the gravity, buoyancy and hydrodynamic forces on the submersible. The velocity value at the current depth is calculated according to Eq. (2). Subsequently, the depth value is increased in set steps and the calculation process described above is repeated to obtain the velocity values at different depths.

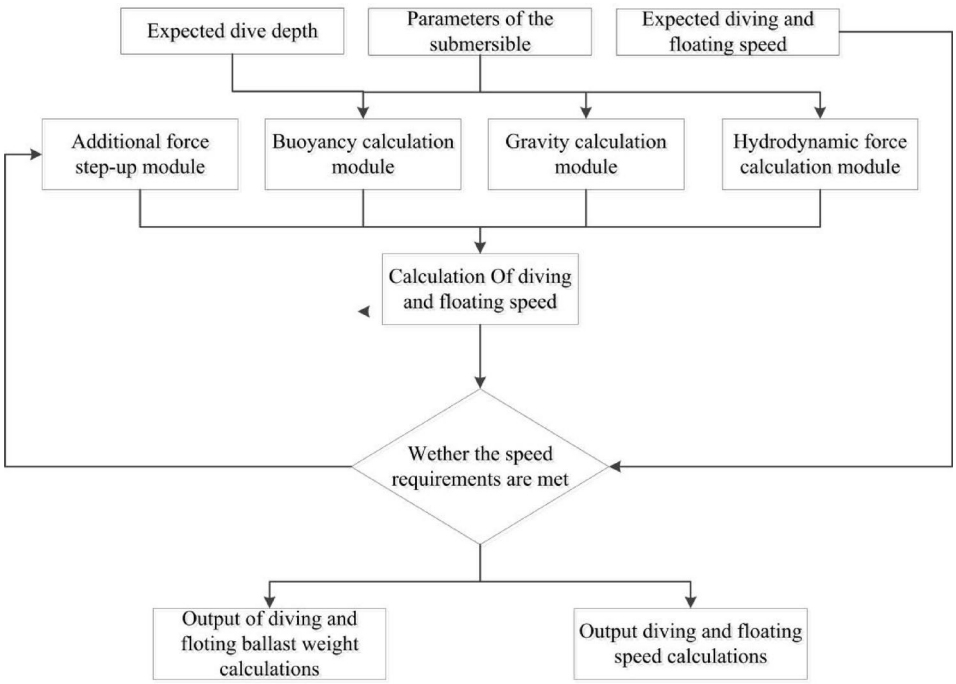

Fig. 10. Overall calculation flow.

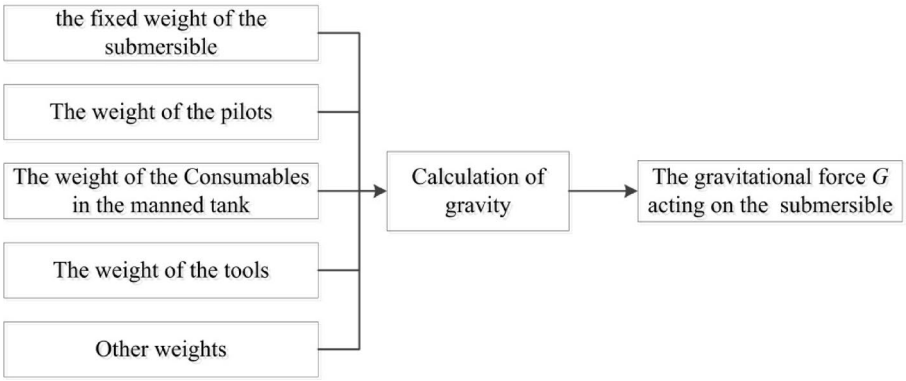

Fig. 11. Calculation flow of gravity.

Parameters	Parameter usage
The fixed weight of the submersible	This parameter is utilised for the purpose of calculating the fixed weight M_0 of the submersible
The weight of pilots	These parameters are utilised for the purpose of calculating the variable weight M_C of the submersible
The weight of consumables in the manned tank	
The weight of tools	
Other weights	

Table 1. The parameters necessary to calculate the gravity force.

The mean value of the speed is calculated and compared with the expected speed to ascertain whether the speed is as expected.

The calculation of the gravity force on the submersible is illustrated in Fig. 11.

The parameters necessary to calculate the gravity force on the submersible are enumerated in Table 1. The parameters needed to calculate gravity include the fixed and variable weight of the submersible. The variable weights include the weight of pilots, the weight of consumables in the manned compartment, the weight of tools and other weights. Utilising the aforementioned calculation parameters as inputs and Eq. (3), the gravity force on the manned submersible can be calculated (Fig. 11).

The calculation of the buoyancy force on the submersible is illustrated in Fig. 12.

The parameters necessary to calculate the buoyancy force on the submersible are enumerated in Table 2. The parameters needed to calculate buoyancy force include the displaced volume when the manned submersible is completely submerged at the start of the dive at the sea surface, the current depth of the submersible, the primary parameters of the spherical shell pressure-resistant bodies, the primary parameters of the cylindrical shell pressure-resistant bodies, the primary parameters of the buoyant material and the primary parameters of the pressure-compensating component. Utilising the aforementioned calculation parameters as inputs and Section "Calculation of the displaced volume loss coefficient", the displaced volume loss coefficient k on the manned submersible can be calculated. Combined with parameters such as the current depth of the submersible and the displaced volume when the manned submersible is completely submerged at the start of the dive at the sea surface, the buoyancy force on the submersible at the current depth can be calculated (Fig. 12).

The calculation of the hydrodynamic force on the submersible is illustrated in Fig. 13.

The parameters necessary to calculate the hydrodynamic force on the submersible are enumerated in Table 3. The parameters needed to calculate hydrodynamic force include the current depth of the submersible, The feature length, The drag coefficient(include diving phase and floating phase) and the velocity at current depth.

Computational validation

Taking the "Jiao Long" manned submersible and the "Shen Hai Yong Shi" manned submersible as the research objects, according to the submersible parameters in the literature[21] and the literature[25], and using the method described in this paper, we carry out matching calculations of the weights of the unpowered diving ballast and floating ballast of the manned submersible, predict the unpowered diving and floating motion, and compare them with the sea trial data.

"Jiao Long" manned submersible

The principal parameters of the "Jiao Long" manned submersible are documented in the extant literature[21]. The primary parameters of the submersible are outlined in Table 4. In Table 4, h is used to denote the depth at which the manned submersible is currently located.

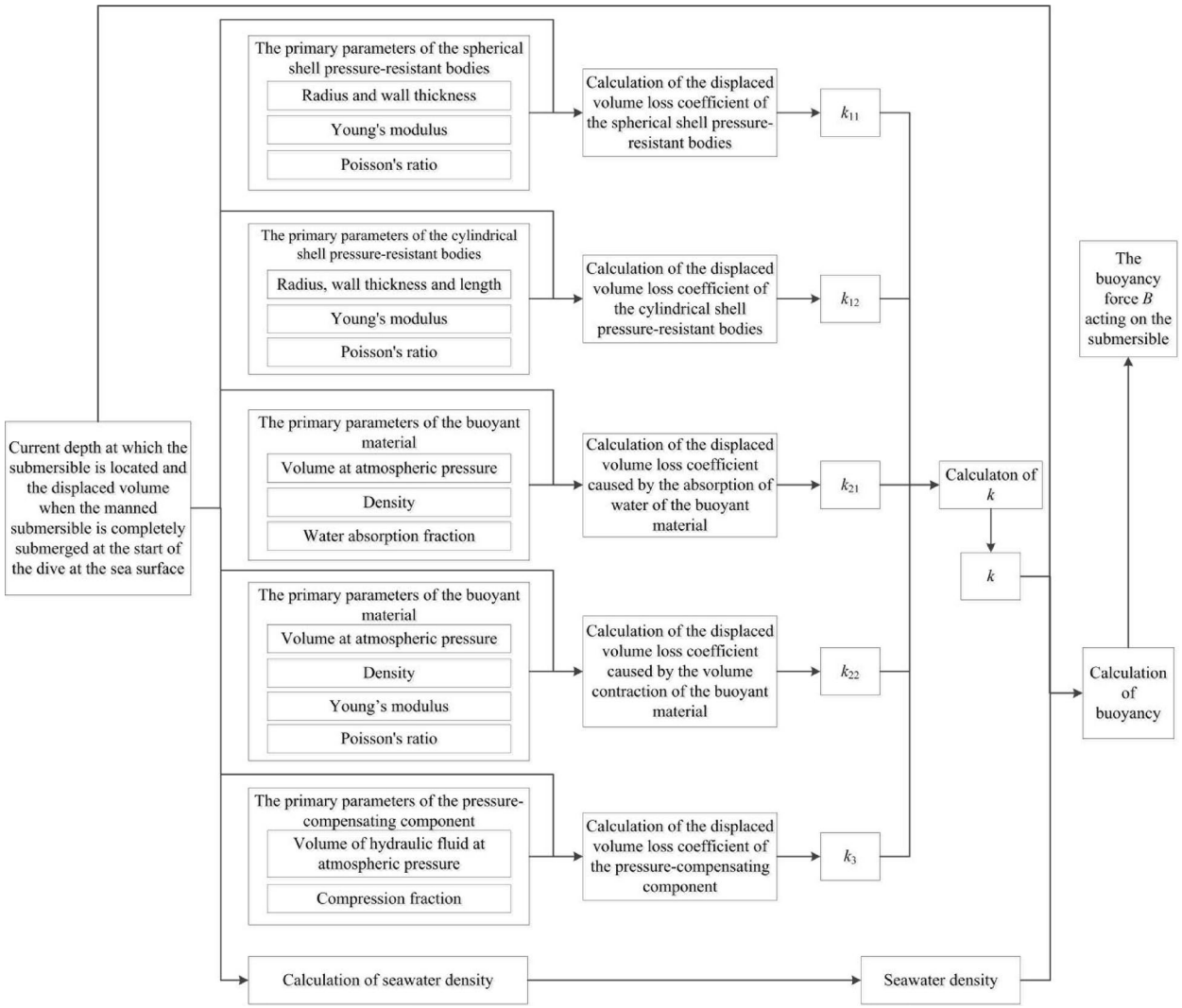

Fig. 12. Calculation flow of buoyancy.

Dive 44 at 5000 m

For the 44th dive to 5000 m, the payload parameters of the "Jiao Long" manned submersible are shown in Table 5.

The objectives of the diving and floating motions of the "Jiao Long" manned submersible are shown in Table 6.

We used the method described in this paper to match the weights of diving ballast and floating ballast for the 44th dive of the "Jiao Long" manned submersible and to forecast the diving and floating motions. The results of the calculation of the weights of the diving ballast and floating ballast are shown in Table 7.

As shown in Table 7, the calculated weights of both the diving ballast and the floating ballast exceed the test results. In particular, the weight of the diving ballast is 8.9% greater than the test results, the weight of the floating ballast is 1.1% greater than the test results, and the total weight of the diving ballast and floating ballasts is 3.6% greater than the test results.

The results of the diving and floating motion predictions are presented in Fig. 14. The results of the prediction demonstrate a high degree of consistency between the predicted diving and floating velocities and the corresponding results of the sea trial.

Dive 50 at 7000 m

For the 50th dive to 5000 m, the payload parameters of the "Jiao Long" manned submersible are shown in Table 8.

The objectives of the diving and floating motions of the "Jiao Long" manned submersible are shown in Table 9.

We used the method described in this paper to match the weights of diving ballast and floating ballast for the 50th dive of the "Jiao Long" manned submersible and to forecast the diving and floating motions. The results of the calculation of the weights of the diving ballast and floating ballast are shown in Table 10.

As shown in Table 10, the calculated weights of both the diving ballast and the floating ballast are less than the test results. In particular, the weight of the diving ballast is 6.5% smaller than the test results, the weight of the

Parameters		Parameter usage
The displaced volume when the manned submersible is completely submerged at the start of the dive at the sea surface V_0		This parameter is utilised for the purpose of calculating the displaced volume loss coefficient k
The current depth of the submersible h		This parameter is utilised for the purpose of calculating process parameters such as seawater pressure and seawater density, derived from the current depth
The primary parameters of The spherical shell pressure-resistant bodies	Radius R	These parameters are utilised for the purpose of calculating the displaced volume loss coefficient k_{11} of the spherical shell pressure-resistant bodies
	Wall thickness t	
	Young's modulus E	
	Poisson's ratio μ	
The primary parameters of the cylindrical shell pressure-resistant bodies	Radius r	These parameters are utilised for the purpose of calculating the displaced volume loss coefficient k_{12} of the cylindrical shell pressure-resistant bodies
	Wall thickness t	
	Length l	
	Young's modulus E	
	Poisson's ratio μ	
The primary parameters of the buoyant material	Volume at atmospheric pressure V_{bm0}	These parameters are utilised for the purpose of calculating the displaced volume loss coefficient k_{21} caused by the absorption of water of the buoyant material and the displaced volume loss coefficient k_{22} caused by the volume contraction of the buoyant material
	Density ρ_{bm}	
	Water absorption fraction η	These parameters are utilised for the purpose of calculating the displaced volume loss coefficient k_{21} caused by the absorption of water of the buoyant material
	Young's modulus E	These parameters are utilised for the purpose of calculating the displaced volume loss coefficient k_{22} caused by the volume contraction of the buoyant material
	Poisson's ratio μ	
The primary parameters of the pressure-compensating component	Volume of hydraulic fluid at atmospheric pressure V_{hf0}	These parameters are utilised for the purpose of calculating the displaced volume loss coefficient of the pressure-compensating component k_3
	Compression fraction η_{hf}	

Table 2. The parameters necessary to calculate the buoyancy force.

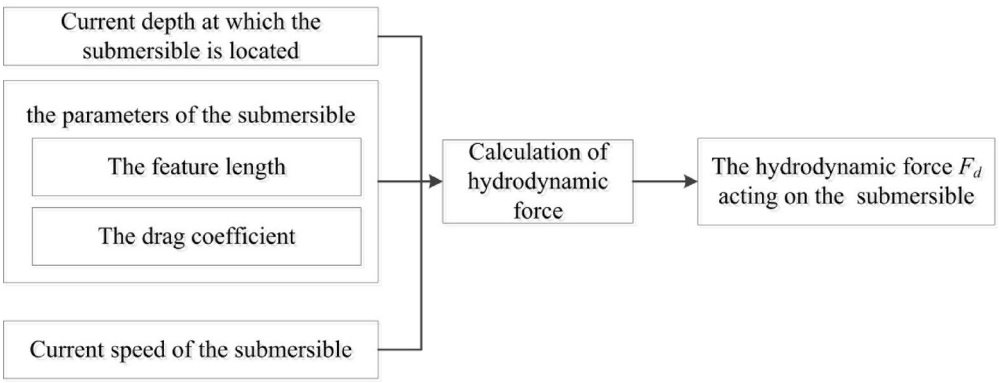

Fig. 13. Calculation flow of hydrodynamic force.

Parameters	Parameter usage
The current depth of the submersible h	This parameter is utilised for the purpose of calculating process parameters such as seawater density, derived from the current depth
The feature length L	These parameters are utilised for the purpose of calculating the hydrodynamic force
The drag coefficient C_z(include diving phase and floating phase)	
Velocity at current depth U	This parameter under consideration is the one for which a solution is being sought. The velocity of the submersible at varying depths is calculated according to the Eq. (2). Subsequently, the mean value of the speed is calculated and compared with the expected speed to ascertain whether the speed is as expected

Table 3. The parameters necessary to calculate the hydrodynamic force.

Parameter term	Value
The fixed weight M_0	20,414 kg
The fixed displaced volume V_0	20.8047 m^3
The feature length L	8.2 m
The drag coefficient C_z	0.28 (diving phase), 0.26 (floating phase)
k_1	3.65×10^{-7} h
k_2	2.23×10^{-6} h
k_3	2.67×10^{-7} h

Table 4. The primary parameters of the "Jiao Long" manned submersible.

Payload term	Weights (kg)	Displaced volume (m^3)
Lead blocks for equalization	203	0.0174
Consumables in the manned tank	35	0
Pilots	224	0
Ballast water	176	0
Tools	35	0.0588

Table 5. The payload parameters of dive 44.

Parameters	Value
Diving depth	5000 m
Average speed of diving	36.6 m/min
Average speed of floating	33.9 m/min

Table 6. Goals of dive 44.

	Calculation (kg)	Sea trial data (kg)	Inaccuracies (%)
Diving ballast	268	246	8.9
Floating ballast	546	540	1.1

Table 7. Comparison of ballast calculations with sea trial data for dive 44.

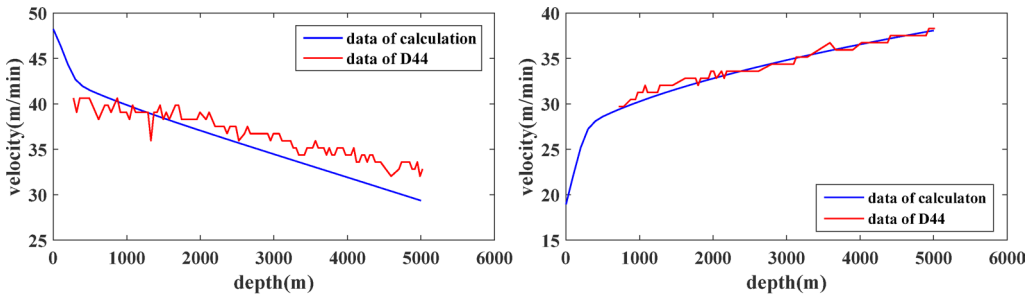

(a) Diving speed (b)Floating speed

Fig. 14. Velocity forecasts during dive 44.

Payload term	Weights (kg)	Displaced volume (m^3)
Lead blocks for equalization	203	0.0174
Consumables in the manned tank	35	0
Pilots	224	0
Ballast water	176	0
Tools	35	0.0588

Table 8. The payload parameters of dive 50.

Parameters	Value
Diving depth	7000 m
Average speed of diving	36.3 m/min
Average speed of floating	34.3 m/min

Table 9. Goals of dive 50.

	Calculation (kg)	Sea trial data (kg)	Inaccuracies (%)
Diving ballast	230	246	− 6.5
Floating ballast	599	600	− 0.2

Table 10. Comparison of ballast calculations with sea trial data for dive 50.

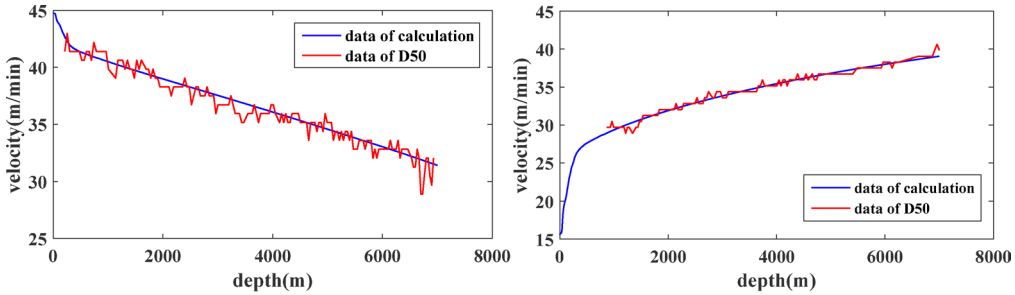

(a) Diving speed (b)Floating speed

Fig. 15. Velocity forecast during dive 50.

floating ballast is 0.2% smaller than the test results, and the total weight of the diving ballast and floating ballasts is 1.8% smaller than the test results.

The results of the diving and floating motion predictions are presented in Fig. 15. The results of the prediction demonstrate a high degree of consistency between the predicted diving and floating velocities and the corresponding results of the sea trial.

"Shen Hai Yong Shi" manned submersible

The principal parameters of the "Shen Hai Yong Shi" manned submersible are documented in the extant literature[25]. The primary parameters of the submersible are outlined in Table 11. In Table 8, h is used to denote the depth at which the manned submersible is currently located.

Dive 17 at 3500 m

For the 17th dive to 3500 m, the payload parameters of the "Shen Hai Yong Shi" manned submersible are shown in Table 12.

The objectives of the diving and floating motions of the "Shen Hai Yong Shi" manned submersible are shown in Table 13.

We used the method described in this paper to match the weights of diving ballast and floating ballast for the 17th dive of the "Shen Hai Yong Shi" manned submersible and to forecast the diving and floating motions. The results of the calculation of the weights of the diving ballast and floating ballast are shown in Table 14.

Parameter term	Value
The fixed weight M_0	18,876.6 kg
The fixed displaced volume V_0	19.4238 m^3
The feature length L	7.5 m
C_z	0.24 (diving phase), 0.23(floating phase)
k_1	5.26×10^{-7} h
k_2	2.59×10^{-6} h
k_3	2.84×10^{-7} h

Table 11. The primary parameters of the "Shen Hai Yong Shi" manned submersible.

Payload term	Weights (kg)	Displaced volume (m^3)
Lead blocks for equalization	16	0
Consumables in the manned tank	54.55	0
Pilots	252	0
Ballast water	0	0
Tools	125	0.0114

Table 12. The payload parameters of dive 17.

Parameters	Value
Diving depth	3500 m
Average speed of diving	36.7 m/min
Average speed of floating	44.4 m/min

Table 13. Goals of dive 17.

	Calculation (kg)	Sea trial data (kg)	Inaccuracies (%)
Diving ballast	249	274	−9.1
Floating ballast	450	454	0.9

Table 14. Comparison of ballast calculations with sea trial data for dive 17.

As shown in Table 14, the calculated weight of the diving ballast is 9.1% less than the results of the sea trial, the calculated weight of the floating ballast is 3.5% greater than the sea trial results, and the total weight of the diving ballast and floating ballast is 2.9% less than the sea trial results.

The results of the diving and floating motion predictions are presented in Fig. 16. The results of the prediction demonstrate a high degree of consistency between the predicted diving and floating velocities and the corresponding results of the sea trial.

Dive 20 at 4500 m

For the 20th dive to 4500 m, the payload parameters of the "Shen Hai Yong Shi" manned submersible are shown in Table 15.

The objectives of the diving and floating motions of the "Shen Hai Yong Shi" manned submersible are shown in Table 16.

We used the method described in this paper to match the weights of diving ballast and floating ballast for the 20th dive of the "Shen Hai Yong Shi" manned submersible and to forecast the diving and floating motions. The results of the calculation of the weights of the diving ballast and floating ballast are shown in Table 17.

As shown in Table 17, the calculated weights of both the diving ballast and the floating ballast are less than the test results. In particular, the weight of the diving ballast is 6.9% smaller than the test results, the weight of the floating ballast is 1.5% smaller than the test results, and the total weight of the diving ballast and floating ballasts is 3.6% smaller than the test results.

The results of the predictive analysis for the diving and floating motions are presented in Fig. 17. The results demonstrate that the predictions regarding the speed of diving and floating are largely in alignment with the findings of the sea trial. As evidenced by the operational record, the manned submersible utilized the propellers within the range of 1600–800 m during the floating process, resulting in a notable shift in the test results for floating speed within the aforementioned range.

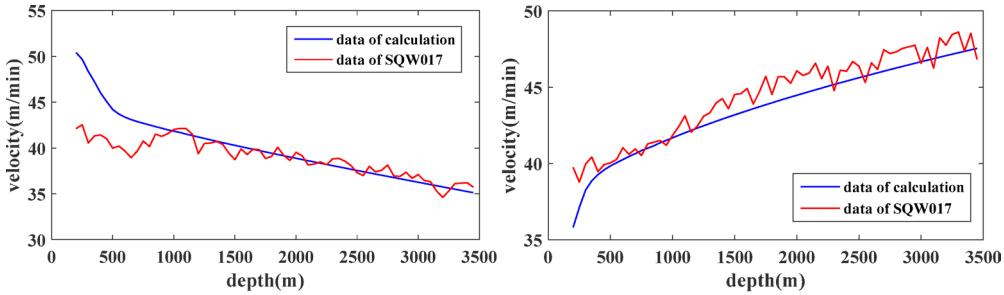

(a) Diving speed (b)Floating speed

Fig. 16. Velocity forecasts during dive 17.

Payload term	Weights (kg)	Displaced volume (m^3)
Lead blocks for equalization	16	0
Consumables in the manned tank	54.55	0
Pilots	238	0
Ballast water	0	0
Tools	158	0.0155

Table 15. The payload parameters of dive 17.

Parameters	Value
Diving depth	4500 m
Average speed of diving	37.8 m/min
Average speed of floating	43.1 m/min

Table 16. Goals of dive 20.

	Calculation (kg)	Sea trial data (kg)	Inaccuracies (%)
Diving ballast	255	274	− 6.9
Floating ballast	447	454	− 1.5

Table 17. Comparison of ballast calculations with sea trial data for dive 20.

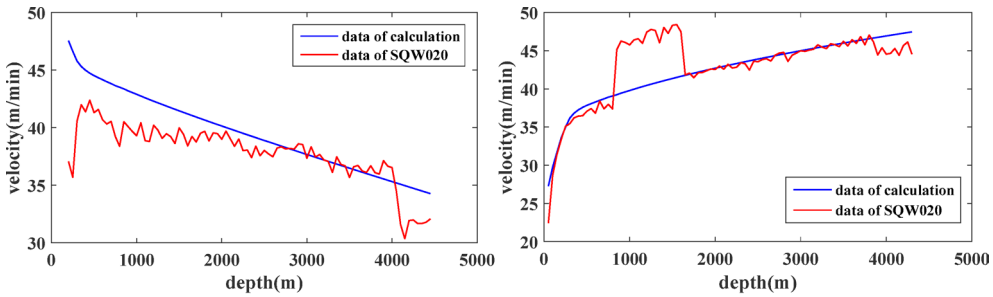

(a) Diving speed (b)Floating speed

Fig. 17. Velocity forecast during dive 20.

Conclusion

This paper presents a mathematical model of the unpowered diving and floating motion of a manned submersible, with a focus on analyzing the forces acting upon the manned submersible. It also outlines a method for computing the ballast required for a deep-sea manned submersible to perform an unpowered dive and float, as well as for predicting the resulting motion. Taking the "Jiao Long" manned submersible and the "Shen Hai Yong Shi" manned submersible as the research objects and using the method described in this paper, we carry out a matching calculation of the weights of the unpowered diving ballast and floating ballast of the manned submersible, predict the unpowered diving and floating motion, and compare them with the sea trial data. The following conclusions may be drawn:

1. It is important to consider the impact of changes in seawater density on the buoyancy forces experienced by a manned submersible, as these changes can significantly influence the forecasting and ballast matching of unpowered diving and floating motions. The EOS80 seawater equation of state is suitable for calculating seawater density at any depth in the ocean.
2. The impact of seawater pressure on the discharge volume of deep-sea manned submersibles is significant and must be considered in unpowered diving ballast and floating ballast-matching calculations and kinematic forecasts for manned submersibles.Displaced volume loss can be classified into three categories: displaced volume loss of pressure-resistant structures, displaced volume loss of buoyant materials, and displaced volume loss of pressure-compensating components.
3. The results of the computational verification demonstrate that the matching results of the weights of the diving ballast and floating ballast obtained via the method described in this paper exhibit a degree of discrepancy with the actual situation. The matching error of the total weights of the diving ballast and floating ballasts is within 4%.The results of the diving and floating motion predictions are largely in alignment with those obtained from sea trials, thereby substantiating the viability and efficacy of the methodology delineated in this paper and demonstrating its suitability for engineering applications.
4. The error can be attributed to several primary factors: ① the effect of attitude changes of the submersible on the unpowered diving and floating motions has not been considered in the mathematical motion modelling. ② The calculation of buoyancy does not consider the variability of the parameters of the marine environment in different seas and seasons. ③ When calculating hydrodynamics, the drag coefficients of submersibles are estimated by empirical formulas, numerical simulation, and modeling tests. These methods, however, are often characterized by limited accuracy. Consequently, subsequent research should be conducted on the aforementioned factors to enhance the calculation method and forecast accuracy.

Data availability

The datasets generated and analyzed during the current study are not publicly available due to workplace and laboratory regulations and confidentiality requirements.

Received: 17 October 2024; Accepted: 30 June 2025
Published online: 10 July 2025

References

1. Cao, J. et al. Current Situation and development of deep-sea submersible equipment. *Shipbuild. China* **61**(1), 204–217 (2020).
2. Sagalevitch A. Experience of the use of manned submersibles in PP Shirshov Institute of Oceanology of Russian Academy of Sciences. In *Proceeding of the 1988 International Symposium on Underwater Technology*, 1988, 403–407. (IEEE, 1988).
3. Sagalevitch, A. From the bathyscaph Trieste to the submersibles Mir. *Mar. Technol. Soc. J.* **43**(5), 79–86 (2009).
4. Nanba, N. et al. Development of deep submergence research vehicle "SHINKAI 6500". *Techn. Rev. Mitsubish Heavy Ind. Ltd* **27**, 157–168 (1990).
5. Momma, H. Deep ocean technology at JAMSTEC. *Mar. Technol. Soc. J.* **33**(4), 49–64 (1999).
6. Cui, W. et al. Introduction to the development of 7000 m manned submersible. *Shipbuild. Shanghai* **1**, 14–17 (2008).
7. Hu, Z. et al. Development of a 4,500-meter manned submersible. *Manag. Res. Sci. Technol. Achiev.* **4**, 50–51 (2019).
8. Liu, T. et al. The current status and technical development of deep sea manned submersible. *Shipbuild. China* **53**(3), 233–243 (2012).
9. Liu, B. et al. Progress of the application and research of manned submersibles used in deep sea scientific investigations. *Haiyang Xuebao* **37**(10), 1–10 (2015).
10. Cui, W. On the development strategy of a full ocean depth manned submersible and its current progress. *J. Jiangsu Univ. Sci. Technol. (Nat. Sci. Ed.)* **29**(1), 1–9 (2015).
11. Xu, W. & Zhang, Q. Overview of present status and development trend of full ocean depth submersibles. *Shipbuild. China* **57**(2), 206–221 (2016).
12. Woods Hole Oceanographic Institution. History of Alvin [EB/OL]. [2023–1–1]. https://www.whoi.edu/what-we-do/explore/underwater-vehicles/hov-alvin/history-of-alvin/.
13. Sagalevitch A. Experience of the use of manned submersibles in PP Shirshov Institute of Oceanology of Russian Academy of Sciences. In *International Symposium on Underwater* (1988).
14. Nanba, N., Marihana, H., Nakamura, E., et al. Development of deep submergence research vehicle "SHINKAI 6500" (1990).
15. Ren, Y. et al. Research on the current status and development trend of manned submersibles. *J. Ocean Technol.* **37**(02), 114–122 (2018).
16. Hardy, K., Sutphen, B. & Cameron, J. Technology of the Deepsea challenge expedition. *Ocean News Technol.* **20**(8), 50–52 (2014).
17. Ye, C., Xu, W. & Liu, S. Application of ergonomics to layout design of manned submersible. *J. Northwestern Polytech. Univ.* **39**(2), 233–240 (2021).
18. Busby, F. Manned Submersibles. Office of the Oceanographer of the Navy, Arlington (1976).
19. Allmendinger, E. E. *Submersible Vehicle Systems Design* (Society of Naval Architects and Marine Engineers, 1990).
20. Zhu, J. *Submersible Design* (Shanghai Jiao Tong University Press, 1992).
21. Pan, B. et al. Development of the unpowered diving and floating prediction system for deep manned submersible "JIAOLONG". *J. Ship Mech.* **16**(z1), 58–71 (2012).

22. Bbeyer, L. A. et al. Measuring gravity on the sea floor in deep water. *J. Geophys. Res.* **71**(8), 2091–2100 (1996).
23. Amos, J. Gravity satellite yields Potato Earth view (2011).
24. Jiang, Y. et al. Gravity and buoyancy analysis of full ocean depth autonomous underwater vehicle. *J. Harbin Eng. Univ.* **41**(4), 481–486 (2020).
25. Hu, Z. et al. Payload calculation for unpowered ascent & descent of manned vehicles. *J. Ship Mech.* **24**(11), 1422–1432 (2020).
26. NODC. World Ocean Atlas 2013 version 2. (NODC, 2013).
27. NODC. World Ocean Database 2013. (NODC, 2013).
28. Li, W. et al. Current status and progress on pressure hull structure of manned deep submersible. *Shipbuild. China* **57**(1), 210–221 (2016).
29. Zhang, Y. Research on Damage Mechanism and Health Monitoring Technology for Key Structural Components of Deep-sea Manned Submarines Structure System. (Harbin Engineering University, 2023).
30. Fan, X. *Stress Analysis and Strength Design of Pressure Vessels* (Atomic Energy Press, 1979).
31. Yang, Z. *Research on Multidisciplinary Optimization Methods for Unmanned Underwater Vehicle Overall Scheme Design* (Harbin Engineering University, 2012).

Author contributions

Conceptualization: H.Z.h, Y.C, Q.W.x. Formal analysis: H.Z.h, Y.C, L.S, Q.W.x. Investigation: H.Z.h, L.S, Q.W.x. Methodology: H.Z.h, Y.C, L.S, Q.W.x. Validation: H.Z.h, L.S, Q.W.x.

Declarations

Competing interests

The authors declare no competing interests.

Additional information

Correspondence and requests for materials should be addressed to Z.H.

Reprints and permissions information is available at www.nature.com/reprints.

Publisher's note Springer Nature remains neutral with regard to jurisdictional claims in published maps and institutional affiliations.